

## Born-Oppenheimer approximation for open quantum systems within the quantum trajectory approach

X. L. Huang(黄晓理),\* S. L. Wu(武松林), L. C. Wang(王林成), and X. X. Yi(衣学喜)†

*School of Physics and Optoelectronic Technology, Dalian University of Technology, Dalian 116024, People's Republic of China*

(Received 4 March 2010; published 17 May 2010; publisher error corrected 27 May 2010)

Using the quantum trajectory approach, we extend the Born-Oppenheimer (BO) approximation from closed to open quantum systems, where the open quantum system is described by a master equation in Lindblad form. The BO approximation is defined and the validity condition is derived. We find that the dissipation in fast variables improves the BO approximation, unlike the dissipation in slow variables. A detailed comparison is presented between this extension and our previous approximation based on the effective Hamiltonian approach [X. L. Huang and X. X. Yi, *Phys. Rev. A* **80**, 032108 (2009)]. Several additional features and advantages are analyzed, which show that the two approximations are complementary to each other. Two examples are described to illustrate our method.

DOI: [10.1103/PhysRevA.81.052113](https://doi.org/10.1103/PhysRevA.81.052113)

PACS number(s): 03.65.Yz, 05.30.Ch

### I. INTRODUCTION

The adiabatic and Born-Oppenheimer (BO) approximations are among the oldest approaches in quantum mechanics [1,2]. The adiabatic approximation [3–8] tells us that, for a time-dependent system governed by the Hamiltonian  $H(t)$ , if the system is prepared in one of the eigenstates  $|n(t=0)\rangle$  of  $H(t=0)$  at  $t=0$ , it will remain in that eigenstate  $|n(t)\rangle$  of  $H(t)$  at arbitrary time  $t > 0$  provided the Hamiltonian  $H(t)$  is changed slowly enough. The Born-Oppenheimer approximation was first given by Born and Oppenheimer in 1927 [2] and can be formulated as follows [9]: Treating the slow variables as parameters, we first solve for the fast variables with fixed slow variables. Using these solutions, we obtain an effective Hamiltonian for the slow variables. This effective Hamiltonian contains an effective vector potential induced by the fast variables. Based on this Hamiltonian we can obtain a wave function with the slow variables. Thus the total wave function can be factorized into a product of two wave functions corresponding to the fast and slow variables. This method has been widely used in physics and quantum chemistry and has become a fundamental tool in these fields [10–22].

Because of the unavoidable coupling of a quantum system to its environment, most quantum systems are open and dissipative [23]. The dynamics of an open quantum system can be described by a master equation [24,25]. It is then natural to ask how these approximations can be extended from closed to open systems. The adiabatic approximation has been extended to open systems in different ways, including the Jordan block method in Liouville space [26,27], the effective Hamiltonian approach [28–30], and in the weak-dissipation limit [31]. Although the approximation based on the effective Hamiltonian approach is equivalent to the Jordan block method [28], the effective Hamiltonian approach has the advantages that the extension is straightforward and the effective Hamiltonian is easy to obtain. The BO approximation was extended based on the effective Hamiltonian approach in

Ref. [32]. In this paper, we shall extend the BO approximation in a different way, based on the quantum trajectory approach. Compared with our previous work, this extension exhibits the following additional features and advantages. (1) We do not need to extend the Hilbert space. This will save CPU (computing) time and memory. (2) All eigenstates of the effective Hamiltonian in the method are physical states. (3) The eigenstates are easy to obtain. (4) The jump terms can be more accurately treated in the master equation than in our previous method. This paper is organized as follows. In Sec. II, we present a general description about our extension and then two examples are given in Sec. III. A detailed comparison between this extension and our previous paper [32] and the conclusions are presented in Sec. IV.

### II. GENERAL TREATMENT

Consider a quantum system with two types of variable, a slow one  $\vec{X}$  and a fast one  $\vec{Y}$ . Then we can divide the total Hamiltonian of the system  $H$  into two parts

$$H = H_s(\vec{X}) + H_f(\vec{X}, \vec{Y}), \quad (1)$$

where  $H_s(\vec{X})$  contains only the slow variables  $\vec{X}$ . The two types of degrees of freedom are coupled together through  $H_f(\vec{X}, \vec{Y})$ . We start by considering dissipation in the fast variables first. The case of decoherence in the slow variables will be discussed later. Assuming the dissipation is in the Lindblad form, the dynamics for such a system can be described by

$$\frac{\partial}{\partial t} \rho = -\frac{i}{\hbar} [H, \rho] + \mathcal{L} \rho, \quad (2)$$

where the first term on the right-hand side represents a unitary evolution while the second term denotes the dissipation. Here we assume that the dissipative term can be arranged into the Lindblad form as

$$\mathcal{L} \rho = \frac{1}{2} \sum_k (2L_k \rho L_k^\dagger - \rho L_k^\dagger L_k - L_k^\dagger L_k \rho), \quad (3)$$

where  $L_k = L_k(\vec{Y})$  is the Lindblad operator relevant to the fast variables  $\vec{Y}$ .  $L_k \rho L_k^\dagger$  denotes the jump term. Within the frame

\*ghost820521@163.com

†yixx@dlut.edu.cn

of the quantum trajectory approach, for an initial state  $|\phi(t_0)\rangle$ , one can write the state after an infinitesimal time  $dt$  as

$$\rho(t_0 + dt) = \left(1 - \sum_k dp_k\right) |\phi_0\rangle\langle\phi_0| + \sum_k dp_k |\phi_k\rangle\langle\phi_k|, \quad (4)$$

where  $dp_k = \langle\phi(t_0)|L_k^\dagger L_k|\phi(t_0)\rangle dt$ , and the new states are defined by

$$|\phi_0\rangle = \frac{(1 - iH_{\text{eff}}dt/\hbar)|\phi(t_0)\rangle}{\sqrt{1 - \sum_k dp_k}}, \quad (5)$$

$$|\phi_k\rangle = \frac{L_k|\phi(t_0)\rangle}{\|L_k|\phi(t_0)\rangle\|},$$

with the non-Hermitian effective Hamiltonian defined by  $H_{\text{eff}} = H - (i/2)\hbar \sum_k L_k^\dagger L_k$ . In this description, the system will jump into the state  $|\phi_k\rangle$  with probability  $dp_k$ , and evolve according to the non-Hermitian effective Hamiltonian  $H_{\text{eff}}$  with probability  $1 - \sum_k dp_k$ . This unraveling is the so-called Monte Carlo wave function method [33–35]. The difficulty here is that the non-Hermitian Hamiltonian  $H_{\text{eff}}$  contains two types of variable; we will solve this problem by applying the BO approximation in the no-jump trajectory only. For the no-jump evolution  $|\phi_0\rangle$ , the time evolution is given by

$$i\hbar \frac{d}{dt} |\Psi(t)\rangle = H_{\text{eff}} |\Psi(t)\rangle. \quad (6)$$

Our aim is to solve this equation with the help of the BO approximation. To this end, we first rewrite  $H_{\text{eff}}$  as  $H_{\text{eff}} = H_s(\vec{X}) + H'_f(\vec{X}, \vec{Y})$  with  $H'_f(\vec{X}, \vec{Y}) = H_f(\vec{X}, \vec{Y}) - (i/2)\sum_k L_k^\dagger L_k$ . Obviously,  $H'_f(\vec{X}, \vec{Y})$  is not Hermitian and it includes all non-Hermitian parts of  $H_{\text{eff}}$ . Taking the slow variables  $\vec{X}$  as parameters, we can solve for the eigenstates of  $H'_f(\vec{X}, \vec{Y})$ . We denote its right eigenstates by  $|\psi_n^R(\vec{X})\rangle$  and the corresponding left eigenstates by  $\langle\psi_n^L(\vec{X})|$  with complex eigenvalues  $E_n(\vec{X})$ . These eigenstates satisfy the relations  $\langle\psi_m^L|\psi_n^R\rangle = \delta_{mn}$  and  $\langle\psi_n^R|\psi_n^R\rangle = 1$  for fixed  $\vec{X}$ . We also restrict our discussion to the nondegenerate case. In order to solve Eq. (6), we expand the eigenstate of  $H_{\text{eff}}$  in terms of  $|\psi_n^R(\vec{X})\rangle$  as

$$|\Phi\rangle = \sum_{n=1}^N c_n |\varphi_n(\vec{X})\rangle |\psi_n^R(\vec{X}, \vec{Y})\rangle, \quad (7)$$

where  $N$  is the dimension of the fast variables  $\vec{Y}$  and  $c_n$  ( $n = 1, 2, 3, \dots, N$ ) are the expansion coefficients. Substituting Eq. (7) into the eigenvalue equation  $H_{\text{eff}}|\Phi\rangle = E|\Phi\rangle$ , after simple calculation, we obtain an equation for the wave function of the slow variables:

$$\sum_m \langle\psi_n^L|H_s(\vec{X})|\psi_m^R\rangle |\varphi_m(\vec{X})\rangle + E_n(\vec{X}) |\varphi_n(\vec{X})\rangle = E |\varphi_n(\vec{X})\rangle. \quad (8)$$

Defining  $H_{n,m}(\vec{X}) = \langle\psi_n^L|H_s(\vec{X})|\psi_m^R\rangle$ , we can rewrite Eq. (8) in matrix form as

$$(\mathcal{H}_0 + \mathcal{H}_P)\varphi = E\varphi, \quad (9)$$

where  $\mathcal{H}_0, \mathcal{H}_P$ , and  $\varphi$  are defined by

$$\mathcal{H}_0 = \begin{bmatrix} H_1 + E_1(\vec{X}) & 0 & \cdots & 0 \\ 0 & H_2 + E_2(\vec{X}) & \cdots & 0 \\ \vdots & \vdots & \ddots & \vdots \\ 0 & 0 & \cdots & H_N + E_N(\vec{X}) \end{bmatrix}, \quad (10)$$

$$\mathcal{H}_P = \begin{bmatrix} 0 & H_{1,2} & \cdots & H_{1,N} \\ H_{2,1} & 0 & \cdots & H_{2,N} \\ \vdots & \vdots & \ddots & \vdots \\ H_{N,1} & H_{N,2} & \cdots & 0 \end{bmatrix}, \quad \varphi = \begin{bmatrix} |\varphi_1\rangle \\ |\varphi_2\rangle \\ \vdots \\ |\varphi_n\rangle \end{bmatrix}.$$

Here we have omitted repeated subscripts for simplicity. Treating  $\mathcal{H}_P$  as a perturbation, we can solve Eq. (9) by virtue of the standard time-independent perturbation theory. The solution to zero order,

$$\tilde{\varphi}_{1,k}^{R[0]} = \begin{bmatrix} |\varphi_{1,k}^{R[0]}\rangle \\ 0 \\ \vdots \\ 0 \end{bmatrix}, \quad \tilde{\varphi}_{2,k}^{R[0]} = \begin{bmatrix} 0 \\ |\varphi_{2,k}^{R[0]}\rangle \\ \vdots \\ 0 \end{bmatrix}, \quad (11)$$

$$\cdots, \cdots, \tilde{\varphi}_{N,k}^{R[0]} = \begin{bmatrix} 0 \\ 0 \\ \vdots \\ |\varphi_{N,k}^{R[0]}\rangle \end{bmatrix},$$

can be obtained by the eigenvalue equation

$$\mathcal{H}_n |\varphi_{n,k}^{R[0]}\rangle = E_{n,k}^{[0]} |\varphi_{n,k}^{R[0]}\rangle, \quad (12)$$

where  $\mathcal{H}_n = H_n(\vec{X}) + E_n(\vec{X})$  is the zero-order effective Hamiltonian for the slow variables. From these zeroth-order solutions, one can obtain the higher-order correction. The condition with which we can neglect the higher-order correction safely is

$$\left| \frac{\langle\varphi_{n',k'}^{L[0]}|H_{n',n}|\varphi_{n,k}^{R[0]}\rangle}{E_{n',k'}^{[0]} - E_{n,k}^{[0]}} \right| \ll 1 \quad \text{for all } k', n' \neq k, n, \quad (13)$$

where  $\langle\varphi_{n',k'}^{L[0]}|$  is the left eigenstate of the non-Hermitian Hamiltonian  $\mathcal{H}_n$ .

Next we consider the dissipation of the slow variables. The method used in this case is very similar to the discussion given above. In this case, the Lindblad operator is replaced by  $X_k$  and it is a function of slow variables only, that is,  $X_k = X_k(\vec{X})$ . In the no-jump trajectory, we divide the non-Hermitian Hamiltonian as  $H_{\text{eff}} = H'_s(\vec{X}) + H_f(\vec{X}, \vec{Y})$ , where  $H'_s(\vec{X}) = H_s(\vec{X}) - (i/2)\sum_k X_k^\dagger X_k$ . The method used to find the eigenstates and eigenvalues for  $H_f$  is the same as for a closed system. These eigenstates are denoted by  $|\psi_n(\vec{X})\rangle$  with corresponding eigenvalues  $E_n(\vec{X})$ . We can handle the slow variables in the same way. The only difference is  $H_{n,m}(\vec{X})$  in Eq. (8), defined as  $H_{n,m}(\vec{X}) = \langle\psi_n|[H_s(\vec{X}) - (i/2)\sum_k X_k^\dagger X_k]|\psi_m\rangle$ . The zero-order effective Hamiltonian  $\mathcal{H}_n$  for slow variables in the no-jump trajectory can be similarly obtained. Compared with the closed system, this Hamiltonian

includes a non-Hermitian (usually anti-Hermitian) correction  $\langle \psi_n | - (i/2) \sum_k X_k^\dagger X_k | \psi_n \rangle$ , which comes from the dissipation.

According to the previous discussion, we can solve the dynamics governed by the non-Hermitian Hamiltonian  $H_{\text{eff}}$  via expanding the total state as  $|\Phi\rangle = \sum_{n,k} c_{n,k} |\varphi_{n,k}^{[0]}\rangle |\psi_n^{(R)}\rangle$ . Then the Monte Carlo simulation for Eq. (2) is the following. We divide the total evolution time  $T$  into several steps. The interval of each step is  $dt$ . In each step, a random number  $\varepsilon$  that is distributed uniformly in the unit interval  $[0,1]$  is chosen to determine the jump process. If  $\varepsilon \leq \sum_k dp_k$ , the total state jumps into the corresponding state according to the corresponding Lindblad operator, that is, for  $\varepsilon \leq dp_1$ , it jumps to  $|\phi_1\rangle$ , for  $dp_1 < \varepsilon \leq dp_1 + dp_2$ , it jumps to  $|\phi_2\rangle$ , and so on. If  $\varepsilon > \sum_k dp_k$ , it is a no-jump process. The system evolves according to the non-Hermitian Hamiltonian  $H_{\text{eff}}$ , and the BO approximation is used. This process is repeated as many time as  $n_{\text{step}} = T/dt$ , and this single evolution gives a quantum trajectory. We can recover the final state of the system by averaging over different quantum trajectories.

### III. EXAMPLES

In this section, we shall present two examples to illustrate our method. After these two examples, we will give a detailed comparison with our previous work [32]. First, we consider a Fabry-Perot (FP) cavity with an oscillating mirror at one end, acting as a quantum-mechanical harmonic oscillator (see Fig. 1). Such a system can be described by the Hamiltonian

$$H = \hbar\omega a^\dagger a - \hbar\chi a^\dagger a x + \frac{p^2}{2m} + \frac{1}{2}m\Omega^2 x^2, \quad (14)$$

where  $\omega$  is the frequency of the cavity field with the creation and annihilation operators  $a^\dagger$  and  $a$ , respectively.  $m$ ,  $\Omega$ ,  $x$ , and  $p$  denote the mass, frequency, displacement, and momentum of the oscillating mirror, respectively.  $\chi = \omega/L$  is the coupling constant between the cavity field and the mirror.  $L$  denotes the length of the cavity. When the cavity dissipation is taken into account, the Lindblad operator in this example is  $L_1 = \sqrt{\gamma}a$ . The non-Hermitian effective Hamiltonian for the no-jump trajectory can be written as

$$H_{\text{eff}} = \hbar \left( \omega - \frac{i}{2}\gamma \right) a^\dagger a - \hbar g a^\dagger a (b + b^\dagger) + \hbar \Omega \left( b^\dagger b + \frac{1}{2} \right), \quad (15)$$

where  $b = \sqrt{m\Omega/2\hbar}(x + ip/m\Omega)$  and  $g = \chi\sqrt{\hbar/2m\Omega}$ . Usually, the characteristic frequency of the cavity field can

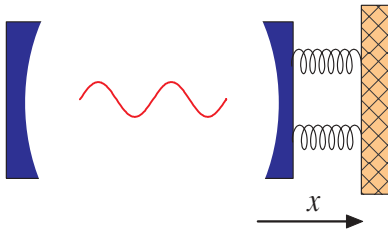


FIG. 1. (Color online) Schematic illustration of a Fabry-Perot cavity with an oscillating mirror at the right end.

reach the order of about  $10^{14}$  Hz, which is much higher than the nanomechanical resonator frequency  $10^9$  Hz achieved in current experiments [12]. Under this condition, we can divide this Hamiltonian into two parts as  $H_{\text{eff}} = H_s + H_f$ , with  $H_s = \hbar\Omega(b^\dagger b + \frac{1}{2})$  and  $H_f = \hbar(\omega - \frac{1}{2}i\gamma)a^\dagger a - \hbar g a^\dagger a (b + b^\dagger)$ . The eigenstate for the fast variables  $H_f$  is  $|\psi_{n_a}^R\rangle = |n_a\rangle$ , where  $|n_a\rangle$  is the Fock state for the mode  $a$ , and the corresponding left eigenstate  $\langle \psi_{n_a}^L | = \langle n_a |$  and eigenvalue  $E_{n_a} = \hbar(\omega - i\gamma)n_a - \hbar g n_a (b + b^\dagger)$ . Putting these into Eq. (12) and following the BO approximation process, we obtain the Hamiltonian for the slow variables as

$$\mathcal{H}_{n_a} = \hbar\Omega(b^\dagger b + \frac{1}{2}) - \hbar g n_a (b + b^\dagger) + \hbar(\omega - \frac{1}{2}i\gamma)n_a. \quad (16)$$

This Hamiltonian can be solved by a displacement of the Fock state [12] as

$$|\varphi_{n_a, n_b}^R\rangle = D(\alpha(n_a))|n_b\rangle, \\ E_{n_a, n_b} = \hbar\Omega \left( n_b + \frac{1}{2} \right) + \hbar \left( \omega - \frac{1}{2}i\gamma \right) n_a - \frac{\hbar g^2}{\Omega} n_a^2,$$

where  $D(\alpha) = e^{A^\dagger \alpha - A \alpha^*}$  is the displacement operator with  $A = b - \alpha$ ,  $\alpha(n_a) = n_a g / \Omega$ , and  $|n_b\rangle$  is the Fock state for mode  $b$ . Note that, in this model, the off-diagonal elements of the perturbation  $\mathcal{H}_p$  are zero, so the BO solution  $|\varphi_{n_a, n_b}^R\rangle$  for the no-jump trajectory is an exact solution. We study the dynamics for such a Hamiltonian according to the method given above and compare this solution to the solution obtained by the Runge-Kutta method in Fig. 2. We choose  $|\Phi(0)\rangle = \frac{1}{2}(|0\rangle + |1\rangle)(|0\rangle + |1\rangle)$  as the initial state. To make the effects of dissipation more striking, we choose the parameters as  $\omega = 100\Omega$ ,  $g = 0.1\Omega$  in the simulation. In Fig. 2(a) we study the entanglement between the vibration of the mirror and the cavity field. We choose negativity [36] as the measure of entanglement for mixed states. In the simulation, the density matrix is calculated by averaging over different runs, that is, from the state vectors  $|\psi_i(t)\rangle$  for the different trajectories, the density

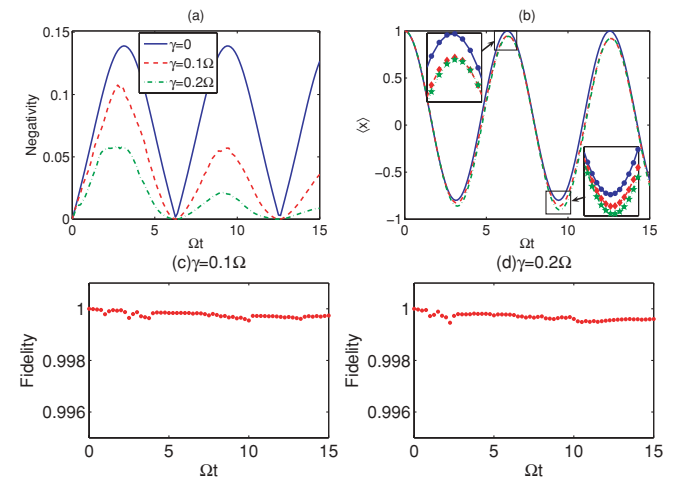


FIG. 2. (Color online) (a) Entanglement measured by the negativity as a function of  $\Omega t$ . (b) Average value of the coordinate  $\langle x \rangle$  (in units of  $\sqrt{\hbar/2m\Omega}$ ) as a function of  $\Omega t$ . (c),(d) Fidelity between the quantum trajectory solution and numerical simulation (Runge-Kutta method). Other parameters in the simulation are  $\omega = 100\Omega$  and  $g = 0.1\Omega$ . The results are obtained by averaging over  $\mathcal{N} = 150$  runs.

matrix can be constructed as  $\rho(t) = (1/N) \sum_i^N |\psi_i(t)\rangle\langle\psi_i(t)|$ . Then we can calculate the negativity for  $\rho(t)$ . We find that the Hamiltonian Eq. (14) can produce entanglement. The dissipation decreases the entanglement gradually, and the larger is the dissipation, the more quickly the entanglement decays. In Fig. 2(b) we plot the average value of the coordinate  $x$  for the oscillating mirror as a function of  $\Omega t$ . From the figure, we see that when the system is closed, the average value of the coordinate for the mirror oscillates with time. The dissipation moves the curve left. Similarly, the strength of the dissipation determines the displacement. In our simulation, we average our results over  $\mathcal{N} = 150$  runs. To check the validity of our method, we compare our results with the results from the Runge-Kutta method. We use the fidelity [37] as the measure of the difference between two density matrices. For a mixed state, the fidelity is defined as  $F(\rho_1, \rho_2) = \text{Tr} \sqrt{\sqrt{\rho_1} \rho_2 \sqrt{\rho_1}}$ . This fidelity reaches 1 when the two states are the same. In Figs. 2(c) and 2(d), we plot the fidelity between the BO solution and the Runge-Kutta solution as a function of  $\Omega t$  for different  $\gamma$ . It is obvious that the fidelities are always larger than 99.9% in our simulation for  $\mathcal{N} = 150$  trajectories.<sup>1</sup> The error is smaller than 0.1%. This confirms that our method can reproduce the dissipation dynamics for open systems efficiently.

Next we briefly discuss the dissipation in the slow variables for this model. In this case, we also assume that the dissipation is in the Lindblad form; the Lindblad operator reads  $X_1 = \sqrt{\kappa}b$ , and the non-Hermitian effective Hamiltonian for the no-jump trajectory is

$$H_{\text{eff}} = \hbar\omega a^\dagger a - \hbar g a^\dagger a (b + b^\dagger) + \hbar\Omega (b^\dagger b + \frac{1}{2}) - \frac{1}{2} i \hbar \kappa b^\dagger b. \quad (17)$$

We divide it into two parts as  $H_{\text{eff}} = H_s + H_f$  with  $H_s = \hbar\Omega (b^\dagger b + \frac{1}{2}) - \frac{1}{2} i \hbar \kappa b^\dagger b$  and  $H_f = \hbar\omega a^\dagger a - \hbar g a^\dagger a (b + b^\dagger)$ . The eigenstates for the fast variables are  $|\psi\rangle = |n_a\rangle$  with eigenvalues  $E_{n_a} = \hbar\omega n_a - \hbar g n_a (b + b^\dagger)$ . With this knowledge, we obtain the zero-order effective Hamiltonian for the slow variables as

$$\mathcal{H}_{n_a} = \hbar\Omega_0 (b^\dagger b + \frac{1}{2}) - \hbar g n_a (b + b^\dagger) + \hbar\omega n_a + \frac{1}{2} i \hbar \kappa \quad (18)$$

with  $\hbar\Omega_0 = \hbar\Omega - \frac{1}{2} i \hbar \kappa$ . This Hamiltonian can be solved in a similar way with the displacement  $\alpha_0 = n_a g / \Omega_0$ . The calculations are similar to the process where the dissipation in fast variables is taken into account. The numerical results

<sup>1</sup>The convergence velocity of the Monte Carlo wave function method depends on the problem considered, that is, the number of jump operators. Moreover, for different operators, the number of runs  $\mathcal{N}$  with which we can get a good result depends on the properties of the operators themselves. For global operators, we can get good results with a relatively small number of runs. This is discussed in detail in Ref. [34]. In our example, the time for the Runge-Kutta solution is as much as about  $\mathcal{N} = 50$  runs for the Monte Carlo wave function method. In our simulation, if  $\mathcal{N} = 25$ , the fidelity can reach 99%; if  $\mathcal{N} = 50$ , that is, the times for both methods are equivalent, the fidelity is higher than 99.5%. The reason for setting  $\mathcal{N} = 150$  in our simulation is to get a fidelity higher than 99.9%.

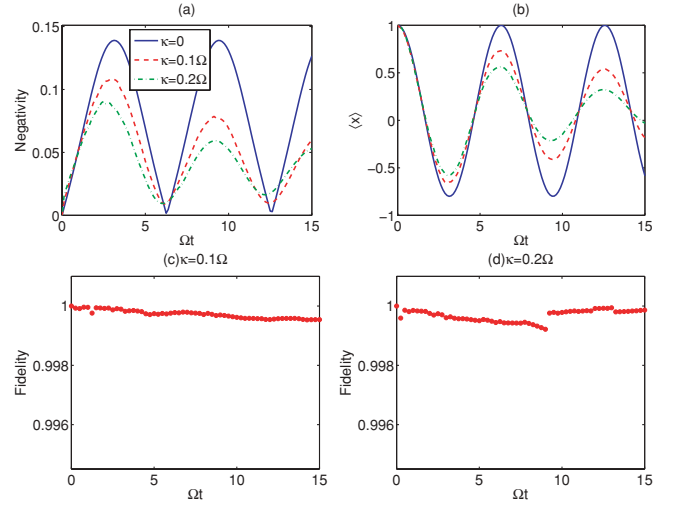


FIG. 3. (Color online) As Fig. 2 for dissipation in slow variables.

for this case is shown in Fig. 3. Two differences can be seen from the figure: (1) When the dissipation in slow variables is taken into account, the entanglement never disappears. (2) The amplitude for the average value of the coordinate  $\langle x \rangle$  decreases strikingly because of dissipation. We should note that in this model, the perturbation  $\mathcal{H}_p$  is zero in the dissipation of both the slow and fast variables. In general, this condition cannot be satisfied [see the second example and Eq. (23)]; thus we need to restrict the dissipation in slow variables to be weak, because strong dissipation in the slow variables enlarges the perturbation  $\mathcal{H}_p$ , which breaks the BO condition. This can be understood as follows: a large dissipation rate may accelerate the change of slow variables, so that it is hard to distinguish which are the fast variables.

In the second example, we consider a neutron moving in a static helical magnetic field,

$$\vec{B} = \vec{B}(z) = B \left( \sin \theta \cos \frac{2\pi z}{L}, \sin \theta \sin \frac{2\pi z}{L}, \cos \theta \right). \quad (19)$$

The Hamiltonian for such a system is

$$H = H(z) = \frac{\vec{p}^2}{2M} + \mu \vec{B} \cdot \vec{\sigma} = H_K + H_S, \quad (20)$$

where  $\vec{\sigma} = (\sigma^x, \sigma^y, \sigma^z)$  are the Pauli operators. Taking the spin relaxation into account, the Lindblad operator is  $L_2 = \sqrt{\kappa} \sigma^-$ . If the coordinate is treated as a parameter, the non-Hermitian Hamiltonian for the no-jump trajectory can be written as

$$H_{\text{eff}} = \mu \vec{B} \cdot \vec{\sigma} - \frac{1}{2} i \hbar \kappa \sigma^+ \sigma^- \\ = \mu B \begin{pmatrix} \cos \theta - \frac{1}{2} i g & \sin \theta e^{-2\pi z i / L} \\ \sin \theta e^{2\pi z i / L} & -\cos \theta \end{pmatrix}, \quad (21)$$

where  $g = \kappa \hbar / \mu B$  is the dimensionless dissipation rate. For each fixed  $z$ , this non-Hermitian Hamiltonian has two right eigenstates,

$$|\psi_+^R\rangle = \frac{1}{N} \left( \cos \frac{\alpha}{2} |1\rangle + \sin \frac{\alpha}{2} e^{2\pi z i / L} |0\rangle \right), \\ |\psi_-^R\rangle = \frac{1}{N} \left( \sin \frac{\alpha}{2} |1\rangle - \cos \frac{\alpha}{2} e^{2\pi z i / L} |0\rangle \right),$$

two left eigenstates

$$\begin{aligned} \langle \psi_+^L | &= N \left( \cos \frac{\alpha}{2} \langle 1 | + \sin \frac{\alpha}{2} e^{-2\pi zi/L} \langle 0 | \right), \\ \langle \psi_-^L | &= N \left( \sin \frac{\alpha}{2} \langle 1 | - \cos \frac{\alpha}{2} e^{-2\pi zi/L} \langle 0 | \right), \end{aligned}$$

and corresponding eigenvalues (in units of  $\mu B$ )

$$E_{\pm} = -\frac{1}{2}ig \pm \frac{1}{2}\sqrt{16 - g^2 - 8ig \cos \theta}.$$

In these expressions, the angle  $\alpha$  is defined as

$$\tan \alpha = \frac{4 \sin \theta}{4 \cos \theta - ig},$$

and the normalized coefficient  $N$  is

$$N = \sqrt{\left| \cos \frac{\alpha}{2} \right|^2 + \left| \sin \frac{\alpha}{2} \right|^2}.$$

Note that, for a nonzero dimensionless dissipation rate  $g$ ,  $\alpha$  is a complex number. In this case, the relation  $\sin^2(\alpha/2) + \cos^2(\alpha/2) = 1$  holds while  $|\sin(\alpha/2)|^2 + |\cos(\alpha/2)|^2 = 1$  does not. Putting these eigenstates and eigenvalues into Eq. (12), we obtain the zero-order Hamiltonian for the spatial variables as

$$\begin{aligned} \mathcal{H}_n &= -\frac{\hbar^2}{2M}(\vec{\nabla} - i\vec{A}_n)^2 + E_n, \\ \vec{A}_n &= i\langle \psi_n^L | \vec{\nabla} | \psi_n^R \rangle, \quad n = +, -. \end{aligned} \quad (22)$$

With this knowledge, we study the population transfer among the internal states for the quantum system. Suppose that we prepare the spin of the neutron in the state  $|+\frac{1}{2}\rangle$  initially and manipulate the particle, moving it from  $z = 0$  to  $z = L$  in a fixed time interval  $T = 3$  (in units of  $\pi\hbar/\mu B$ ). Setting  $\theta = \pi/4$ , we study the polarization of the neutron along the  $z$  axis versus time  $t$  with different dimensionless dissipation rate  $g$ ; the results are shown in Fig. 4. In the simulation we take  $\mathcal{N} = 400$  trajectories. Some features can be seen from the figure: When dissipation is absent, the polarization along the  $z$  axis oscillates between 0 and 1 as a cosine function of time. The dissipation leads the polarization damping to  $-1$

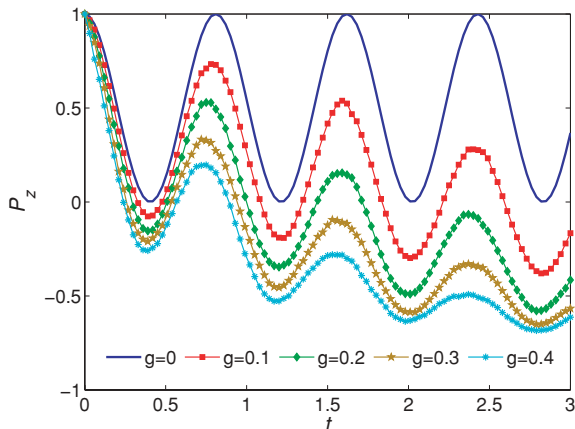


FIG. 4. (Color online) Polarization of the neutron along the  $z$  axis as a function of time  $t$  (in units of  $\pi\hbar/\mu B$ ) for different dimensionless dissipation rates  $g$ . We have set  $\theta = \pi/4$  and initially the spin is in the state  $|+\frac{1}{2}\rangle$ .

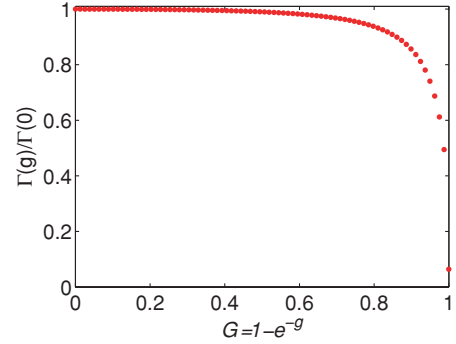


FIG. 5. (Color online) Validity measure  $\Gamma(g)$  as a function of the dimensionless dissipation rate  $g$ . The results have been normalized in units of  $\Gamma(g = 0)$ . Other parameters in the figure are set to satisfy  $\hbar/\mu BM^2L = 10^{-6}$  and  $\hbar k_z/\mu BML = 2 \times 10^{-4}$ .

in an oscillating fashion. The stronger is the dissipation, the faster is the damping. To measure the validity condition, we define a function

$$\Gamma(g) = \max \left( \left| \frac{\langle \varphi_{n',k'}^{L[0]} | O_{n',n} | \varphi_{n,k}^{R[0]} \rangle}{E_{n',k'}^{[0]} - E_{n,k}^{[0]}} \right| \right), \quad (23)$$

where  $O_{n',n} = -(\hbar/2M)(2\langle \psi_{n'}^L | \vec{\nabla} | \psi_n^R \rangle \cdot \vec{\nabla} + \langle \psi_{n'}^L | \nabla^2 | \psi_n^R \rangle)$ , to characterize the violation of the BO condition. From Fig. 5 we can see that the spin relaxation improves the approximation. This is the same result as that in our previous work [28,32], and it can also be understood in that dissipation in the fast variables improves the approximation, because it accelerates the movement of fast variables, and the difference between the two types of variable becomes more evident.

#### IV. DISCUSSIONS AND CONCLUSIONS

It is time to give a detailed comparison between this method and our previous approach [32]. We note that the differences come from the two methods themselves. These lead to the following distinct features: (1) In Ref. [32], the extension is done by an effective Hamiltonian approach, which requires extension of the Hilbert space. In the present paper, the extension is done according to the quantum trajectory approach which does not require extension of the Hilbert space. In addition, in the present paper, if the initial state is pure, the state will always be pure in its evolution. (2) In the effective Hamiltonian approach, the extension is simple and straightforward; however, the eigenstates of the Hamiltonian, including the fast variables, may not be physical states, although it gives the correct dynamics. For example, the last three eigenstates of  $H_S^T$  in Ref. [32] are not physical states. In the quantum trajectory approach, the eigenstates are all physical states. (3) The complexity is different. The analytical solution for the no-jump trajectory is easier than the effective Hamiltonian solution. For example, the last three eigenstates for the fast variables  $H_S^T$  [32] are a cubic equation, whose solution is complicated. For a high-dimensional open system, the problem become more complicated. But it is relatively easy to solve for the eigenstates in this paper, that is, the non-Hermitian Hamiltonian in the no-jump trajectory

can be solved more easily than the effective Hamiltonian in Ref. [32]. (4) The method in the present paper is more accurate in treating the jump term in the master equation. This can be understood as follows. When the dissipation in slow variables is considered, the nondiagonal elements of the perturbation  $\mathcal{H}_P$  can be divided into two parts as  $H_{n,m} = \langle \psi_n | H_s | \psi_m \rangle - \frac{1}{2} i \sum_k \langle \psi_n | X_k^\dagger X_k | \psi_m \rangle$ . The first part is the same as in a closed system while the second part contains only a term of dissipation. The other part of the dissipation is recovered via the jump process. The quantum trajectory solution is more exact than the effective Hamiltonian solution, in which the perturbation includes all parts of the dissipation. Before closing this paper, we emphasize that all the discussions of both methods are restricted to nondegenerate energy levels, that is, we assume the closed-system Hamiltonian is nondegenerate. However, when the dissipation is taken into account, new degeneracy is introduced [38] in both methods. Thus, in the second example in this paper, even though the original system is nondegenerate, the non-Hermitian Hamiltonian  $H_{\text{eff}}$  can be degenerate at  $\theta = \pi/2$  and  $g = 4$ . In Ref. [32] the

degeneracy occurs at  $\theta = \pi/2$ ,  $z = z^A$ , and  $g = 8$ . Obviously, the degenerate points in the two methods are different, so these two methods are complementary in this sense; in other words, when one method is not available because of degeneracy, we can choose the other method.

In summary, we have extended the BO approximation from a closed to an open system using the quantum trajectory approach. An assumption that the dissipation is in Lindblad form is required. The BO approximation is used in the no-jump trajectory, and the dynamics can be recovered by the Monte Carlo wave function method. As illustrations, we give two examples to detail our method. The results show that our method can reproduce the dissipation dynamics for such systems efficiently. A detailed comparison with our previous work is also given and discussed.

### ACKNOWLEDGMENTS

This work is supported by NSF of China under Grants No. 10775023, No. 10935010, and No. 10905007.

- 
- [1] M. Born and V. Fock, *Z. Phys.* **51**, 165 (1928).  
 [2] M. Born and R. Oppenheimer, *Ann. Phys. (Leipzig)* **389**, 457 (1927).  
 [3] K. P. Marzlin and B. C. Sanders, *Phys. Rev. Lett.* **93**, 160408 (2004); S. Duki, H. Mathur, and O. Narayan, *ibid.* **97**, 128901 (2006); J. Ma, Y. P. Zhang, E. G. Wang, and Biao Wu, *ibid.* **97**, 128902 (2006); K. P. Marzlin and B. C. Sanders, *ibid.* **97**, 128903 (2006).  
 [4] Z. Y. Wu and H. Yang, *Phys. Rev. A* **72**, 012114 (2005).  
 [5] D. M. Tong, K. Singh, L. C. Kwek, and C. H. Oh, *Phys. Rev. Lett.* **95**, 110407 (2005).  
 [6] D. M. Tong, K. Singh, L. C. Kwek, and C. H. Oh, *Phys. Rev. Lett.* **98**, 150402 (2007).  
 [7] R. MacKenzie, A. Morin-Duchesne, H. Paquette, and J. Pinel, *Phys. Rev. A* **76**, 044102 (2007).  
 [8] Y. Zhao, *Phys. Rev. A* **77**, 032109 (2008).  
 [9] C.-P. Sun and M.-L. Ge, *Phys. Rev. D* **41**, 1349 (1990).  
 [10] L. S. Cederbaum, *J. Chem. Phys.* **128**, 124101 (2008).  
 [11] C. C. Shu, J. Yu, K. J. Yuan, W. H. Hu, J. Yang, and S. L. Cong, *Phys. Rev. A* **79**, 023418 (2009).  
 [12] Z. R. Gong, H. Ian, Yu-xi Liu, C. P. Sun, and Franco Nori, *Phys. Rev. A* **80**, 065801 (2009).  
 [13] X. X. Yi, H. Y. Sun, and L. C. Wang, e-print [arXiv:0807.2703](https://arxiv.org/abs/0807.2703).  
 [14] S. Bubin, J. Komasa, M. Stanke, and L. Adamowicz, *J. Chem. Phys.* **131**, 234112 (2009).  
 [15] M. Førre, S. Barmaki, and H. Bachau, *Phys. Rev. Lett.* **102**, 123001 (2009).  
 [16] J. B. Shim, M. S. Hussein, and M. Hentschel, *Phys. Lett. A* **373**, 3536 (2009).  
 [17] B. H. Muskatel, F. Remacle, and R. D. Levine, *Phys. Scr.* **80**, 048101 (2009).  
 [18] D. I. Abramov, *J. Phys. B* **41**, 175201 (2009); A. V. Matveenko, E. O. Alt, and H. Fukuda, *ibid.* **42**, 165003 (2009).  
 [19] A. V. Ruban and I. A. Abrikosov, *Rep. Prog. Phys.* **71**, 046501 (2009).  
 [20] J. J. Hua and B. D. Esry, *Phys. Rev. A* **80**, 013413 (2009).  
 [21] E. Tiemann, H. Knockel, P. Kowalczyk, W. Jastrzebski, A. Pashov, H. Salami, and A. J. Ross, *Phys. Rev. A* **79**, 042716 (2009).  
 [22] H. A. Leth, L. B. Madsen, and K. Mølmer, *Phys. Rev. Lett.* **103**, 183601 (2009).  
 [23] U. Weiss, *Quantum Dissipative Systems* (World Scientific, Singapore, 1993).  
 [24] H. P. Breuer and F. Petruccione, *The Theory of Open Quantum Systems* (Oxford University Press, Oxford, 2002).  
 [25] C. W. Gardiner, *Quantum Noise* (Springer, New York, 2000).  
 [26] M. S. Sarandy and D. A. Lidar, *Phys. Rev. A* **71**, 012331 (2005).  
 [27] M. S. Sarandy and D. A. Lidar, *Phys. Rev. Lett.* **95**, 250503 (2005).  
 [28] X. X. Yi, D. M. Tong, L. C. Kwek, and C. H. Oh, *J. Phys. B* **40**, 281 (2007).  
 [29] D. M. Tong, X. X. Yi, X. J. Fan, L. C. Kwek, and C. H. Oh, *Phys. Lett. A* **372**, 2364 (2008).  
 [30] X. L. Huang, X. X. Yi, Chunfeng Wu, X. L. Feng, S. X. Yu, and C. H. Oh, *Phys. Rev. A* **78**, 062114 (2008).  
 [31] P. Thunström, Johan Åberg, and E. Sjöqvist, *Phys. Rev. A* **72**, 022328 (2005).  
 [32] X. L. Huang and X. X. Yi, *Phys. Rev. A* **80**, 032108 (2009).  
 [33] J. Dalibard, Y. Castin, and K. Mølmer, *Phys. Rev. Lett.* **68**, 580 (1992).  
 [34] K. Mølmer, Y. Castin, and J. Dalibard, *J. Opt. Soc. Am. B* **10**, 524 (1993).  
 [35] H. Carmichael, *An Open Systems Approach to Quantum Optics* (Springer-Verlag, Berlin, 1993).  
 [36] G. Vidal and R. F. Werner, *Phys. Rev. A* **65**, 032314 (2002).  
 [37] D. Bures, *Trans. Am. Math. Soc.* **135**, 199 (1969); A. Uhlmann, *Rep. Math. Phys.* **9**, 273 (1976).  
 [38] B. A. Tay and T. Petrosky, *Phys. Rev. A* **76**, 042102 (2007).